High effective adsorption of organic dyes on magnetic cellulose beads entrapping activated carbon

Xiaogang Luo, Lina Zhang*

Department of Chemistry, Wuhan University, Wuhan 430072, China

ABSTRACT

Maghemite (γ-Fe$_2$O$_3$) nanoparticles were created with a submerged circulation impinging stream reactor (SCISR) from FeCl$_3$·6H$_2$O and FeCl$_2$·4H$_2$O by using precipitation followed by oxidation. Subsequently, by blending cellulose with the Fe$_2$O$_3$ nanoparticles and activated carbon (AC) in 7 wt% NaOH/12 wt% urea aqueous solution pre-cooled to $-12\,^\circ$C, millimeter-scale magnetic cellulose beads, coded as MCB-AC, was fabricated via an optimal dropping technology. The cellulose beads containning Fe$_2$O$_3$ nanoparticles exhibited sensitive magnetic response, and their recovery could facilitate by applying a magnetic field. The adsorption and desorption of the organic dyes on MCB-AC were investigated to evaluate the removal of dyes (methyl orange and methylene blue) with different charges from aqueous solution. Their adsorption kinetics experiments were carried out and the data were well fitted by a pseudo-second-order equation. The results revealed that the MCB-AC sorbent could efficiently adsorb the organic dyes from wastewater, and the used sorbents could be recovered completely. Therefore, we developed a highly efficient sorbent, which were prepared by using simple and "green" process, for the applications on the removal of hazardous materials.

© 2009 Published by Elsevier B.V.

1. Introduction

The treatment of household wastewater and industrial effluents is a challenging topic in environmental science and technology, as control of the water pollution and purification of water [1]. Recently, the removals of the hazardous materials from wastewater have attracted many attentions [2,3]. One of the most successful methods for the removal of organic pollutants is via their adsorption on biosorbent. In this respect, biodegradable polymers (synthetic or natural) are gaining increasing interest. The high cost and regeneration difficulties of synthetic polymer sorbents have compelled researchers to focus on alternative low-cost natural polymeric sorbent [4–6]. Among the polymers, polysaccharides such as chitin [7], alginate [1,8,9], starch, and their derivatives (chitosan and cyclodextrin) [10–13] have been reported. It is noted that sorbent made from natural polymers are biodegradable and biocompatible, leading to the wide applications in the food [14] and drug [15,16] industry fields.
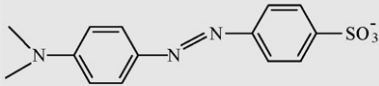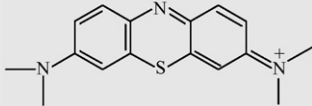
Magnetic separation have been one of the promising ways for an environmental purification technique because of producing no contaminants such as flocculants and having capability of treating large amount of wastewater within a short time [1]. Magnetic nano- or micro-particles of iron oxides have been widely used in the fields of separations and adsorptions, particularly in ion exchange separations [17], enzymes [18] or other proteins, nucleic acids [19] and cell [20] separations, and dyes removal [21,22]. These magnetic nanoparticles embedded in porous polymer materials can expand adsorption capacity due to the improvement in the electrostatic interaction. Activated carbon (AC) is the most commonly absorbent for organic dyes, but the use of AC on a large scale is limited by process engineering difficulties such as the dispersion of the AC powder and the cost of its regeneration. The magnetic properties of iron oxide nanoparticles combined with AC maybe create a new material, which will possess high adsorption capacity and easy recovery through the magnet. The iron oxides and AC powder can be encapsulated in biopolymer beads such as alginate [10] or chitosan [15] to obtain the magnetic sorbent with high adsorption capacity.

Cellulose, the most abundant renewable polysaccharide on earth, is produced by nature at a rate of 10^{11}–10^{12} ton/year [23]. It is noted that cellulose has been used as sorbents for dyes [24,25] and heavy metal [26,27]. The utilization of cellulose as bioaffinity carrier materials should enhance the adsorption capability of organic wastes due to its abundant hydroxyl groups, which give a cationic nature to the biopolymer [15]. Thus, we attempted to develop new cellulose based sorbent for the removal of hazardous materials. In our laboratory, a solvent system for cellulose has been developed, namely 7 wt% NaOH/12 wt% urea aqueous solutions precooled to $-12\,^\circ$C, in which cellulose could dissolve rapidly

* Corresponding author. Tel.: +86 27 87219274; fax: +86 27 68754067.
E-mail address: lnzhang@public.wh.hb.cn (L. Zhang).

Table 1
Structure and properties of dyes.

Dye	Formula	Charge	Molecular weight
Methyl Orange	$C_{14}H_{14}N_3O_3S^- Na^+$	Negative	327.34
Methylene Blue	$C_{16}H_{18}N_3S^+Cl^-$	Positive	373.90

to form a transparent cellulose solution [28]. Moreover, cellulose fibers, magnetic nanocomposite cellulose fibers and porous cellulose microspheres have been prepared from this solution via simple and "green" process [29–31]. However, studies on the magnetic cellulose beads containing iron oxide and AC have never been reported. In present work, we prepared a sorbent, in which the maghemite nanoparticles and AC were embedded in the cellulose matrix to improve the adsorption capacity of organic dyes. Their structure, adsorption behaviors, as well as the desorption and the regeneration properties were investigated to evaluate the desirability of their applications in the water treatment field.

2. Experimental

2.1. Materials

Cotton linter pulp(α-cellulose > 95%) was provided by Hubei Chemical Fiber Group Ltd. (Xiangfan, China). Its viscosity-average molecular weight (M_η) was determined by using an Ubbelohde viscometer in LiOH/urea aqueous solution at $25 \pm 0.05\,°C$ and calculated according to the Mark–Houwink equation [28] $[\eta] = 3.72 \times 10^{-2} M_W^{0.77}$ to be 8.1×10^4.

Activated carbon was purchased from Sigma–Aldrich. The Brunauer–Emmett–Teller (BET) surface area and the total pore volume of AC were determined by using a computer-controlled nitrogen gas adsorption analyzer (ASAP2010) at 77 K to be $1250 \pm 20\,m^2\,g^{-1}$ and $0.66\,mL\,g^{-1}$. AC was sifted through 120-mesh sieve before used.

The negatively charged methyl orange (MO) and positively charged methylene blue (MB) were purchased from Sigma–Aldrich, and were used as received. These dyes were chosen as the model organic dyes for evaluating the adsorption and desorption behaviors of the sorbent. Their chemical structures and properties are listed in Table 1. Stock solutions of dyes were prepared by dissolving the powder in distilled water, and their concentrations were measured by UV spectrophotometer (Shimadzu UV-160A, Japan). The dye solutions with different concentrations were prepared by diluting the stock solution. Other chemicals were of analytical grades, and were purchased in China. The chemicals were used without further purification.

2.2. Preparation of the sorbent

The maghemite (γ-Fe$_2$O$_3$) nanoparticles were fabricated according to a synthetic method described by Massart [32]. Nevertheless, we used a new reactor device, submerged circulative impinging stream reactor (SCISR). The SCISR [33] equipment used was as similar to that of the stagnation jet mixer designed by Brauer [34] shown in Fig. 1. SCISR has a special flow configuration,

resulting in the circulation of perfect-mixing-flow and non-mixing-flow in sequence and in a strong micro-mixing effect in the impingement zone. It provided unique advantages in preparing ultra-fine powders [35] and nanoparticles [36]. The maghemite (γ-Fe$_2$O$_3$) nanoparticles were synthesized by co-precipitation of a stoichiometric mixture of ferrous and ferric chloride in an ammonium hydroxide solution and coated by citrate ions. The resulting magnetite (Fe$_3$O$_4$) precipitates were acidified by nitric acid and oxidized into maghemite (γ-Fe$_2$O$_3$) at $90\,°C$ with iron nitrate. The effective volume of the SCISR used was $3.6 \times 10^{-3}\,M^3$. Concentrated ammonium hydroxide (200 mL, $11\,mol\,L^{-1}$) was added to an acidic aqueous solution of iron (II) chloride and iron (III) chloride ($[Fe_{total}] = 0.13\,mol\,L^{-1}$ with $V_{total} = 3.0\,L$ and $[Fe(II)]/[Fe(III)] = 0.5$) containing 3 g of citric acid trisodium salt at $60\,°C$. The precipitate, consisting of anionic magnetite particles (Fe$_3$O$_4$), was isolated by centrifugation and washed twice with distilled water for 10 min. The precipitate was then stirred in a solution of nitric acid (400 mL, $2\,mol\,L^{-1}$) to obtain the magnetite particles, and then oxidized to maghemite at $90\,°C$ for 30 min by ferric nitrate (600 mL, $0.34\,mol\,L^{-1}$). To prepare the final product, the maghemite nanoparticles were precipitated with acetone, and then were freeze-dried by using a lyophilizer (CHRIST Alpha 1-2, Germany) to give maghemite powders.

A solution mixed with NaOH/urea/H$_2$O of 7:12:81 by weight was cooled to $-12\,°C$, and then 6 g cellulose was immediately dispersed into the solvent (200 mL) under vigorous stirring for 3 min to obtain
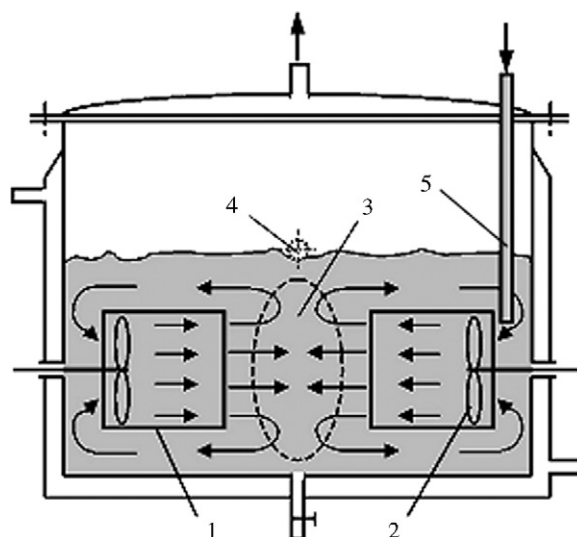
Fig. 1. Schematic structure of SCISR: (1) drawing tube; (2) propeller; (3) impingement zone; (4) outlet; (5) filling tube.

a transparent cellulose solution. 6 g of γ-Fe_2O_3 and 0.5 g of AC powder were added into the cellulose solution with a mechanical stirrer for 1 h. The resulting suspension was added drop wise in a sodium chloride bath (500 mL, 10 wt%) at a constant rate (4.3 mL min^{-1}) by means of a syringe pump. An optimal drop technology with height of 6 cm was used to prepare spherical beads [37,38]. A magnet set under the sodium chloride bath drew the beads out of the dropping zone without having to stir the bath. The beads were cured in the sodium chloride bath overnight. 100 Magnetic cellulose beads with 85.7% of moisture content and 3.8 g of sodium chloride were added into 100 mL of NaOH aqueous solution at −4 °C. After stirring for 30 min, 10 mL of epichlorohydrin was slowly added into the above mixture with stirring for 45 min, and then it was raised to 75 °C with stirring 150 min to obtain the cross-linked cellulose beads. In this case, the Fe_2O_3 nanoparticles were prevented, unable to be removed from the cellulose beads, as a result of the strong interactions of the hydrogen bonding and the electrostatic interaction occurred between the groups of cellulose and Fe_2O_3 [30,39]. The cross-linked beads were washed 5 times with distilled water and kept in water before characterization. Unless specifically noted, no drying process was done and the beads were used in wet state to avoid the collapse of the internal structure [40]. The cross-linked magnetic cellulose beads embedded with Fe_2O_3 and activated carbon were designated as MCB-AC. In the cellulose beads no removal of AC or the magnetic nanoparticles was observed, indicating a strong interaction among cellulose, Fe_2O_3 and AC.

2.3. Characterization

Transmission electron microscopy (TEM) observation was carried out on a JEOL 100 CX2 electron microscope (JEOL, Tokyo, Japan), using an accelerating voltage of 200 kV. A two-parameter fit of the magnetization curves allowed the determination of the mean diameter d_0 ($\ln d_0 = \langle \ln d \rangle$) and the distribution width σ. Wide-angle X-ray diffraction (XRD) measurement was carried out on an XRD diffractometer (D8-Advance, Bruker). The patterns with the Co Kα radiation ($\lambda = 0.15406$ nm) at 40 kV and 30 mA were recorded in the region of 2θ from 35° to 55°. The average crystallite size of the particles was determined from the line width of the (3 1 1) plane reflection, using the Scherer equation. The magnetic properties of the maghemite were studied with a superconducting quantum interference device (SQUID, MPMS XL-7, QUANTUM DESIGN, USA) at 25 °C, and the hysteretic loop was obtained in a magnetic field that varied from −7 to +7 T. Samples were ground into powders and dried in a vacuum oven at 60 °C for 48 h.

The beads were observed and photographed with a digital camera (Canon A630). Digitized photographs of the beads were used in combination with image analysis software (Image J) to obtain their mean diameter and size distribution. To verify the reproducibility of the beads preparation, three different samples (200 beads) were analyzed for each preparation. The observation of the surface structure of the wet beads was carried out on a FESEM scanning electron microscopy (SEM, SIRION TMP, FEI).

2.4. Adsorption experiments

In the dye-cellulose system, the dyes adsorption was driven by the binding enthalpy, which was ascribed to van der Waals forces, and some was driven by entropy [41]. The efficiency of the removal of organic dyes from aqueous solutions by MCB-AC was experimentally studied by recording the adsorption isotherms, kinetic experiments and effects of pH. A known weight of MCB-AC (~5 g) containing 29 mg of AC, 343 mg of cellulose and 343 mg Fe_2O_3, were added to 20 mL of dye solutions in the concentrations range from 0.2 to 2 mmol L^{-1}. The equilibrium pH of the solution was 6.7 ± 0.2 without pH adjustment. After 48 h, the beads were removed from

the solution by magnetic separation using a magnet (0.2 T). The concentration of the organic dyes in the solutions was determined with UV spectrophotometer. The removed quantity (Q_{eq} in mmol g^{-1}, wet beads) of dye by the beads was calculated by

$$Q_{eq} = \frac{C_0 - C_{eq}}{m} V \tag{1}$$

where C_0 (mmol L^{-1}) represents the initial dye concentration, C_{eq} (mmol L^{-1}) is the equilibrium concentration of dye remaining in the solution, V (L) is the volume of the aqueous solution, and m (g) is the weight of wet beads.

Kinetic experiments were performed by using different flasks containing around 5 g of MCB-AC (29 mg AC, 343 mg cellulose and 343 mg maghemite) in 20 mL of the dye solution (1 and 5 mmol L^{-1}). At desired time intervals, the beads were removed from the solution by magnetic separation. The remaining amount of dye in the aqueous solution was then determined by UV spectrophotometery.

To study the effect of pH on the dye removal by MCB-AC, the experiments were carried out at different pH ranging from 3 to 10. Tested samples were prepared by adding MCB-AC (~5 g) to 20 mL of a dye solution (1 mmol L^{-1}). As the pH of the solution became less than 2, the dissolution of the Fe_2O_3 nanoparticles occurred, causing the beads to lose the magnetic properties [1]. pH was adjusted by using concentrated solutions of tetramethylammonium hydroxide or nitric acid, and the pH was regularly measured. After 48 h, the beads were removed with a magnet and the resultant solutions were analyzed.

2.5. Desorption and regeneration experiments

To study the cycle, the previously used MCB-AC was regenerated in the 2 mol L^{-1} NaCl, and then be used in another adsorb test. It could be repeated for many times. To completely regenerate the adsorbent, further regeneration would be required by using the 2 mol L^{-1} NaCl and 0.05 mol L^{-1} NaOH. After elution, the MCB-AC beads were rinsed three times with deionized water to remove any trace of salt and alkaline. The adsorption–desorption cycle was repeated three times by using the same MCB-AC and initial concentration used in this experiment. Desorption efficiency of dyes from the MCB-AC beads was calculated as the ratio of the amount of the desorbed dyes to amount of the adsorbed dyes.

3. Results and discussion

3.1. Structure and size of magnetic nanoparticles

Fig. 2a shows TEM image of the Fe_2O_3 nanoparticles in water. Clearly, the Fe_2O_3 nanoparticles existed as spheres with diameter of about 10 nm. A two-parameter fit of the magnetization curves allowed the determination of the mean diameter ($d_0 = 10$) and the distribution width ($\sigma = 0.4$). Fig. 2b shows the magnetization of the Fe_2O_3 nanoparticles as a function of the applied magnetic field at 298 K. The paramagnetic property of the magnetic particles from the hysteresis loop was measured with a vibrating sample magnetometer (VSM, Lake Shore, 7304, USA), and the saturation magnetization intensity of Fe_2O_3 nanoparticles was about 42.2 emu g^{-1}, and it exhibited an extremely small hysteresis loop. Therefore, the maghemite nanoparticles are expected to respond well to magnetic fields without any permanent magnetization.

The identity and purity of the maghemite nanoparticles were measured by XRD. The XRD pattern of the Fe_2O_3 nanoparticles is shown in Fig. 3. The XRD peaks of the nanocrystallite were matched well with standard γ-Fe_2O_3, and no other crystalline phases were detected. The mean diameter of Fe_2O_3 crystalline was also estimated by Scherer's equation to be 10.2 nm, in good agreement with
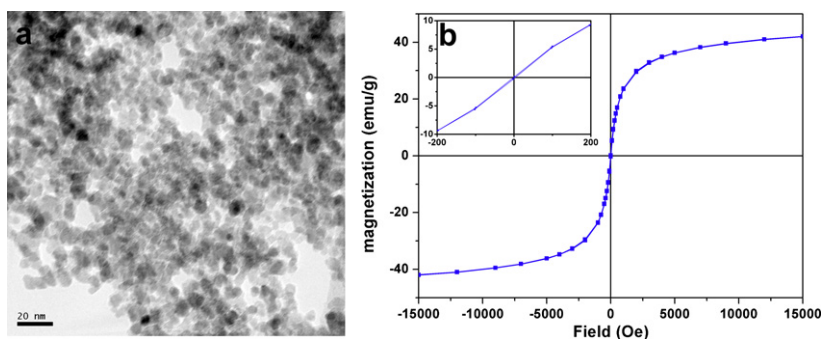
Fig. 2. TEM image of Fe$_2$O$_3$ nanoparticles (a) and magnetization of the Fe$_2$O$_3$ nanoparticles as a function of applied magnetic field at 298 K (b), insert: a magnified view of the −200 to 200 Oe regions.

that measured by TEM. Usually, magnetic particles of less than 30 nm would exhibit superparamagnetic properties [42].

3.2. Morphology and structure of the MCB-AC beads

Fig. 4 shows photograph of the MCB-AC beads attracted by a magnet (a), photograph of beads (b) and the size distribution of the beads (c). The MCB-AC beads were spherical and dark brown due to the presence of γ-Fe$_2$O$_3$ nanoparticles and AC. The spherical beads exhibited uniform and dense surface. The Fe$_2$O$_3$ nanoparticles and AC powders as fillers were added in the cellulose matrix, leading to the formation of the spherical shape structure, as shown in Fig. 4b. The water containing the MCB-AC beads was clear, suggesting that the γ-Fe$_2$O$_3$ nanoparticles and AC were immobilized well in the cellulose matrix. The magnetic beads could be easily removed from the aqueous solution with an addition of magnet, indicating the sensitive magnetic response. The size distribution curve fits a Gaussian distribution is given in Fig. 4c. The mean diameter of the beads and the polydispersity factor were 2.2 mm and 0.06, respectively, indicating a successful fabrication of the cellulose composite beads.

Surface morphology of the wet beads was visualized by SEM (not shown). We observed a creased exterior surface which was different from the smooth and regular surface of pure cellulose beads. This aspect is associated with the presence of inorganic fillers as it was previously observed [31].

In addition, the iron content of the beads (0.21 mmol g^{-1}, wet beads) was close to the amount of magnetic nanoparticles, which were initially added to the cellulose solution (0.21 mmol g^{-1}, wet

beads). It was confirmed that Fe$_2$O$_3$ nanoparticles and AC were embedded strongly in the cellulose matrix, leading to the formation of the composite materials. It is not hard to imagine that a strong interaction existed between Fe$_2$O$_3$, AC particles and cellulose matrix in the MCB-AC beads. By dropping the Fe$_2$O$_3$/AC/cellulose solution into sodium chloride bath with optimal height of 6 cm, the spherical beads were fabricated successfully. Therefore, this work provided a "green" pathway for the preparation of the MCB-AC beads including the γ-Fe$_2$O$_3$ nanoparticles and AC, and this process is promising on a large-scale production.

3.3. Kinetics of the sorption process

The pictures of the adsorption process of the dyes and adsorption amount as function of time are shown in Fig. 5. The dyes MO (a–c) and MB (e and f) could be adsorbed by the MCB-AC within 2 h, leading to the slight color of red or blue. After 3 h, the wastewater changed to be almost colorless. The results indicated that the MCB-AC beads could purify effectively water to remove the organic dyes. The effect of contact time on the removal of MB and MO with an initial concentration of 1 mmol L^{-1} by MCB-AC is presented in Fig. 5d and h. A rapid uptake of the adsorbed amount of the dyes occurred within the first minutes during the adsorption process. About 50% of dye was adsorbed within 22 min for MO and 5 min for MB. The results indicated that the adsorption occurred mainly on the surface of the porous sorbent and driven by the van der Waals force. As mentioned above, the MCB-AC beads have abundant −OH groups and AC with high adsorption capacity as well as large specific surface area, leading to the strong adsorptions potential in the aqueous solution containing the hazardous materials.

From the economical point of view, the contact time required to reach equilibrium is an important parameter for the application of the wastewater treatment. Although there was a small difference in the initial adsorption rates of MO and MB, the equilibrium time was 180 min for both dyes. Several kinetic models are available to study the mechanisms of the sorption process and to fit the experimental data. Among them the pseudo-second-order equation [43] is often successfully used to describe the kinetics of the fixation reaction of pollutants on the adsorbent:

$$\frac{dQ_t}{dt} = k(Q_{eq} - Q_t)^2 \tag{2}$$

where k (g mmol^{-1} min^{-1}) is the second-order rate constant, Q_{eq} (mmol g^{-1}, wet bead) is the amount of dye adsorbed at equilibrium and Q_t (mmol g^{-1}, wet bead) is the amount of dye adsorbed at any time t (min). Integrating this equation with the boundary conditions $t = 0$ ($Q_t = 0$) to t_{eq} ($Q_t = Q_{eq}$) and then linearizing leads to

$$\frac{t}{Q_t} = \frac{1}{kQ_{eq}^2} + \frac{1}{Q_{eq}}t \tag{3}$$
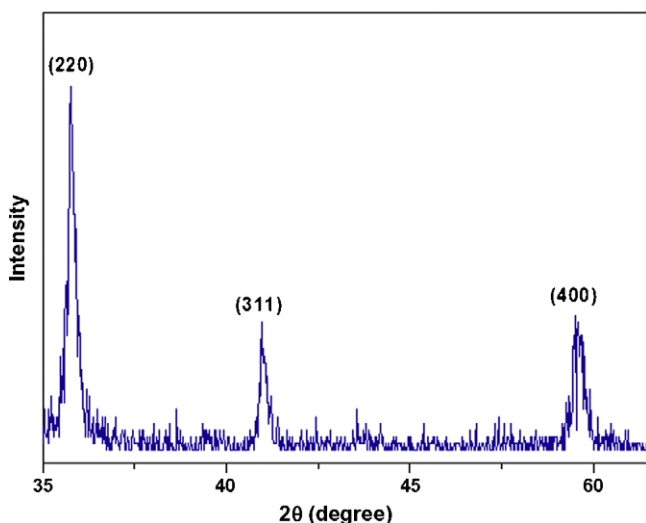
Fig. 3. The powder X-ray diffraction pattern of the Fe$_2$O$_3$ nanoparticles.
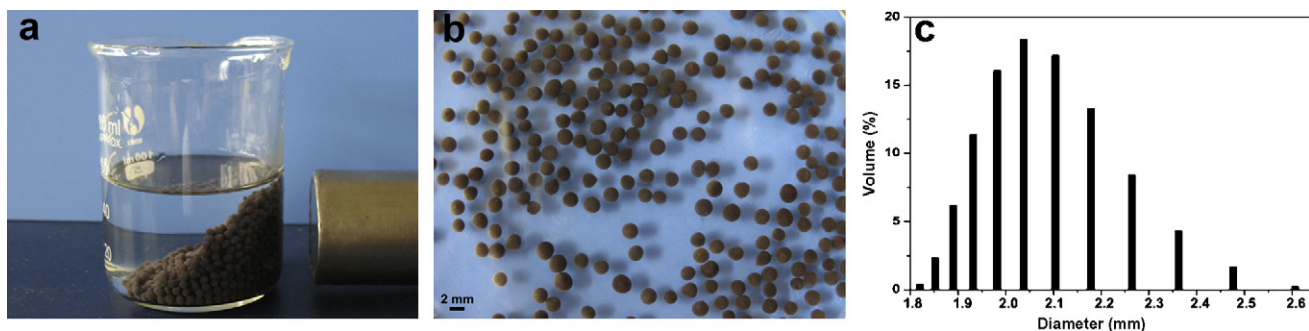
Fig. 4. Photograph of the MCB-AC beads attracted by a magnet (a), photograph of beads (b) and the size distribution of the beads (c).

Table 2
Adsorption kinetic constants modeled by a pseudo-second-order equation (t_{50} presents the time corresponding to 50% of adsorbed dye).

Dye	C_0 (mmol L^{-1})	t_{eq} (min)	$Q_{eq,exp}$ (mmol g^{-1} beads)	$Q_{eq,calc}$ (mmol g^{-1} beads)	k (g mmol^{-1} min^{-1})	t_{50} (min)	R^2
MO	1	180	4.50×10^{-3}	4.00×10^{-3}	9.51	22	0.9984
MB	1	180	2.13×10^{-3}	2.22×10^{-3}	52.65	5	0.9998

The second-order rate constant k and Q_{eq} values were calculated from the slope and intercepts of the t/Q_t versus t plot. A linear relationship with a high correlation coefficients was observed between t/Q_t and t, indicating the applicability of the pseudo-second-order model to describe the sorption process. The correlation coefficients R^2, the second-order constants k and the calculated and experimental equilibrium sorption capacities Q_{eq} are summarized in Table 2. The values of equilibrium sorption capacity showed that a good fit of the experimental curve have been obtained (Fig. 5d and h). The results revealed that the MCB-AC beads possessed high adsorption capacity for MO and MB dyes, and they could selectively and strongly adsorb MO. This could be explained that the presence of AC, Fe$_2$O$_3$ nanoparticles and −OH group of cellulose promoted the dyes with the charges binding into the MCB-AC beads through hydrogen bonds and electrostatic interaction. For subsequent batch experiments, equilibrium time was 5 h, which was more than sufficient to establish equilibrium.

3.4. Adsorption isotherms

A relationship between adsorption capacity of beads and dye concentration can expressed using the Langmuir adsorption equations as

$$\frac{1}{q_e} = \frac{1}{q_{max}} + \frac{1}{q_{max}b} \frac{1}{c_e} \tag{4}$$

and using the Freundlich adsorption equations [44] as
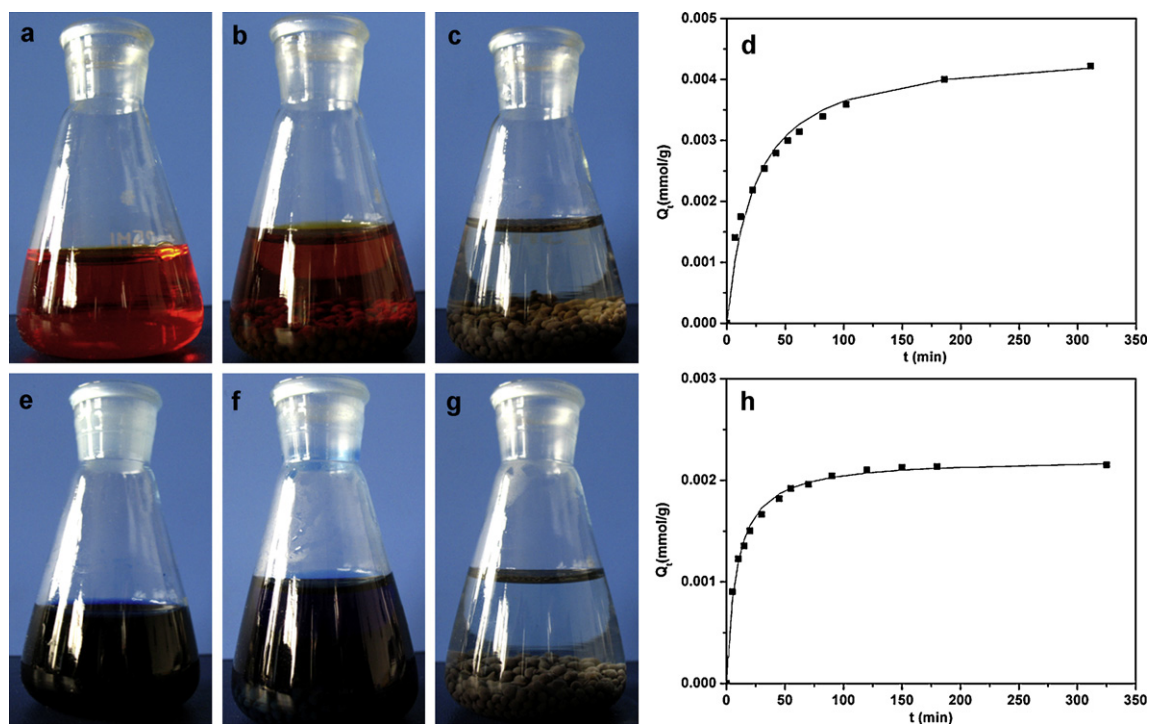
$$\ln q_e = \frac{1}{n} \ln c_e + \ln K_F \tag{5}$$

Fig. 5. The pictures of the adsorption process (left) and adsorbed amount (right) of MO (a–d) and MB (e–h) as a function of time, the full line represents of fit of experimental data with a pseudo second-order kinetics equation.
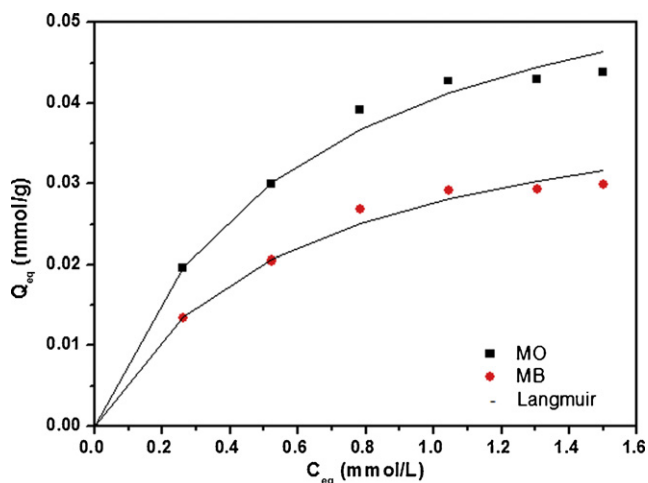
Fig. 6. Comparison of the adsorption equilibria of MO and MB using the Langmuir isotherms.

Fig. 8. Effect of pH on the removal of organic dyes by MCB-AC ($C_0 = 1$ mmol L^{-1}). Q_{eq} is expressed in mmol g^{-1} wet beads.
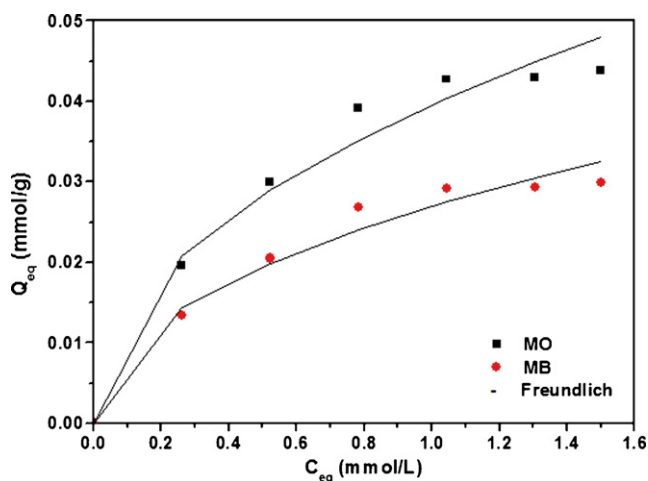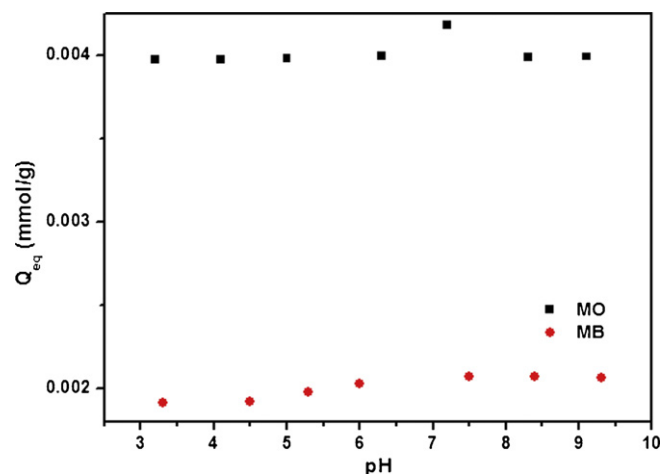

Fig. 7. Comparison of the adsorption equilibria of MO and MB using the Freundlich isotherms.

where q_{max} is the maximum adsorption at monolayer coverage (mmol g^{-1}) and b is the Langmuir adsorption equilibrium constant (mmol L^{-1}), reflecting the energy of adsorption. K_F and $1/n$ are the Freundlich characteristic constants, indicating the adsorption capacity and the adsorption intensity, respectively. The Langmuir isotherm model assumes monolayer adsorption on a surface with a finite number of identical sites, that all sites are energetically equivalent and that there is no interaction between adsorbed molecules. The Freundlich expression is an empirical equation based on adsorption on a heterogeneous surface.

The adsorption isotherm for the MO or MB organics on the MCB-AC beads could be analyzed by both the Langmuir and Freundlich isotherms. Figs. 6 and 7 show the experimental data and Langmuir/Freundlich isotherms for MO and MB on MCB-AC. Table 3 lists the calculated values from Langmuir and Freundlich isothermal

adsorption parameters for the adsorption of the dyes. The MO and MB adsorptive behaviors on MCB-AC could be better represented by the Langmuir equation in the concentration range studied (correlation coefficient, $R^2 > 0.99$). This indicated that the MO and MB organics were adsorbed on the beads as a monolayer adsorption. The Freundlich constant ($1/n$) is related to the sorption intensity of the sorbent. When, $0.1 < 1/n \leq 0.5$, it is easy to adsorb; $0.5 < 1/n \leq 1$, there is some difficult with the absorption; $1/n > 1$, there is quite difficult to adsorb [45]. The $1/n$ value of MO and MB on the beads lied in the range from 0.4 to 0.5 (Table 3), indicating that both of the two dyes could be easily to be adsorbed on the MCB-AC beads. It was noted that both of the correlation coefficient (R^2) for Langmuir and Freundlich indicated significantly correlation. Namely, both Langmuir and Freundlich models could simulate the adsorption equilibrium data of the two dyes in this concentration range. Therefore, it was regarded as physical adsorption combined with effect of chemical adsorption. The parameter q_{max} values gave approximate evaluation of the adsorption amount of MO and MB on the beads. It was revealed that the MCB-AC beads exhibited high adsorption capacity for the organic dyes, similar to those of other similar magnetic adsorbent [1].

The influence of pH on the removal of dyes by MCB-AC was studied to gain further insight into the adsorption process. Fig. 8 shows the effect of pH on the removal of MO and MB by the MCB-AC beads. No significant influence of pH on dye removal was observed for the two organic dyes at the initial concentration (1 mmol L^{-1}). This result confirmed that the adsorption was mainly as a result of the contribution of the encapsulated AC, which is not pH-sensitive. Therefore, AC played an important role in the improvement of the adsorption capacity of the MCB-AC beads. It was worth noting that the MCB-AC beads had higher adsorption capacity for MO than for MB. This revealed that the negatively charged MO was easier to bind with the beads through hydrogen bonds and electrostatic interactions [13]. So the MCB-AC system could adsorb more strongly the negatively charge organic dyes (MO) than positively charged MB, indicating a selective adsorption behavior.

Table 3
Langmuir and Freundlich isothermal adsorption equation parameters for the adsorption of MO and MB.

Dye	Langmuir parameters			Freundlich parameters		
	q_{max} (mmol g^{-1})	b (mmol L^{-1})	R^2	$1/n$	K_F (mmol g^{-1})	R^2
MO	6.48×10^{-3}	0.5970	0.9906	0.4772	3.95×10^{-3}	0.9421
MB	4.39×10^{-3}	0.5880	0.9903	0.4683	2.70×10^{-3}	0.9407

Table 4
Regenerative functions of the adsorbents.

Recycling times	1	2	3
MO (removal efficiencies, %)	99.8	98.4	96.1
MB (removal efficiencies, %)	99.2	97.8	95.5

3.5. Desorption and regeneration

Regenerative functions of the adsorbents are summarized in Table 4. In the first cycle, there were almost no decreases in the sorption capacities. However, the sorption capacities decreased with increasing number of cycles. After three cycles of adsorption-elution, the adsorption capacity was regained completely and the desorption efficiency of dye was maintained at around 95%. The results indicated that the MCB-AC beads loaded with the organic dyes could be regenerated, and be used repeatedly many times.

As shown in Fig. 4, the magnetic beads have sensitive magnetic response in the magnetic field. It is not hard to imagine that the used sorbent can be recycled easily from the wastewater through the magnetic field. This is very important for the industrial application to avoid the secondary pollution in the wastewater treatment.

4. Conclusion

Magnemite (γ-Fe_2O_3) nanoparticles with about 10 nm were created in a submerged circulation impinging stream reactor (SCISR). The magnetic nanoparticles and activated carbon were embedded in cellulose matrix to fabricate a sorbent via simple and "green" process. Two dyes including positively charged MB and negatively charged MO as models of organic dyes were adsorbed effectively by the MCB-AC beads. The Fe_2O_3 nanoparticles and AC in the MCB-AC could play important roles in both the formation of spherical shape beads and the improvement of the adsorption capacity. The MCB-AC beads exhibited high adsorption capacity for the two dyes, and could more strongly adsorb MO. The adsorption kinetics was fast with 180 min to reach equilibrium time, and the kinetic data were well fitted by a pseudo-second-order model. Furthermore, the sorbent could be regenerated and used repeatedly. The magnetic properties of the beads allow their separation from the effluent by applying a magnetic field, leading to the development of a clean and safe process for water pollution remediation. This work provided a new pathway for the preparation of the MCB-AC beads including the γ-Fe_2O_3 nanoparticles and AC, and this process is promising on a large-scale production.

Acknowledgments

References

[1] V. Rocher, J.M. Siaugue, V. Cabuil, A. Bee, Removal of organic dyes by magnetic alginate beads, Water Res. 42 (2008) 1290–1298.
[2] Z. Zhang, S. Xia, A. Yang, B. Xu, L. Chen, Z. Zhu, J. Zhao, J.R. Jaffrezic, D. Leonard, A novel biosorbent for dye removal: extracellular polymeric substance (EPS) of Proteus mirabilis TJ-1, J. Hazard. Mater. 15 (2009) 279–284.
[3] C.H. Niu, B. Volesky, D. Cleiman, Bisorption of arsenic (V) with acid-washed crab scheels, Water Res. 42 (2007) 2473–2478.
[4] S.R. Blackbum, Natural polysaccharides and their interactions with dye molecules: applications in effluent treatment, Environ. Sci. Technol. 38 (2004) 4905–4909.
[5] M.T. Uddin, M.A. Islam, S. Mahmud, M. Rukanuzzaman, Adsorptive removal of methylene blue by tea waste, J. Hazard. Mater. 15 (2009) 53–60.
[6] P. Francesca, M. Sara, New biosorbent materials for heavy metal removal: product development guided by active site characterization, Water Res. 42 (2008) 2953–2962.
[7] E. Guibal, M. Van Vooren, B. Dempsey, J. Roussy, A review of the use of chitosan for the removal of particulate and dissolved contaminants, J. Sep. Sci. Technol. 41 (2006) 2487–2514.
[8] Y.-B. Lin, B. Fugestsu, N. Terui, S. Tanaka, Removal of organic compounds by alginate gel beads with entrapped activated carbon, J. Hazard. Mater. 120 (2005) 237–241.
[9] A.F. Ngomsik, A. Bee, J. Siaugue, V. Cabuil, G. Cote, Nickel adsorption by magnetic alginate microcapsules containing an extractant, Water Res. 9 (2006) 1848–1856.
[10] Y. Sağ, Y. Aktay, Mass transfer and equilibrium studies for the sorption of chromium ions onto chitin, Process Biochem. 36 (2000) 157–173.
[11] G. Crini, Recent developments in polysaccharide-based materials used as adsorbents in wastewater treatment, Prog. Polym. Sci. 30 (2005) 38–70.
[12] H. Yi, L. Wu, W.E. Bentley, R. Ghodssi, G.W. Rubloff, J.N. Culver, G.F. Payne, Biofabrication with chitosan, Biomacromolecules 6 (2005) 2881–2894.
[13] N.K. Lazaridis, G.Z. Kyzas, A.A. Vassiliou, D.N. Bikiaris, Chitosan derivatives as biosorbents for basic dyes, Langmuir 23 (2007) 7634–7643.
[14] G. Crini, Non-conventional low-cost adsorbents for dye removal: a review, Bioresour. Technol. 97 (2006) 1061–1085.
[15] G. Ronca, L. Palmieri, S. Maltiniti, D. Tagliazucchi, A. Conte, Relationship between iron and protein content of dishes and polyphenol content in accompanying wines, Drugs Exp. Clin. Res. 29 (2003) 271–286.
[16] A. Bhatnagar, A.K. Minocha, Conventional and non-conventional adsorbents for removal of pollutants from water: a review, Indian J. Chem. Technol. 13 (2006), 230–127.
[17] M. Sari, S. Akgol, M. Karatas, A. Denizli, Reversible immobilization of catalase by metal chelate affinity interaction on magnetic beads, Ind. Eng. Chem. Res. 45 (2006), 3036–3034.
[18] H. Chen, M. Kaminski, X. Liu, M. Torno, A novel human detoxification system based on nanoscale bioengineering and magnetic separation techniques, Med. Hypotheses 68 (2007) 1071–1079.
[19] J. Akutsu, Y. Tojo, O. Segawa, K. Obata, M. Okochi, H. Tajima, M. Yohda, Development of an integrated automation system with a magnetic bead-mediated nucleic acid purification device for genetic analysis and gene manipulation, Biotechnol. Bioeng. 86 (2004) 667–671.
[20] G. Morstyn, S. William, Cell Therapy: Stem Cell Transplantation, Gene Therapy, and Cellular Immunotherapy, West Nyack, New York, U.S.A., Cambridge University Press, Cambridge, 1996.
[21] N. Yang, S. Zhu, D. Zhang, S. Xu, Synthesis and properties of magnetic Fe_3O_4-activated carbon nanocomposite particles for dye removal, Mater. Lett. 62 (2008) 645–647.
[22] A.A. Atia, A.M. Donia, W.A. Al-Amrani, Adsorption/desorption behavior of acid orange 10 on magnetic silica modified with amine groups, Chem. Eng. J. 1 (2009) 55–62.
[23] D.N.-S. Hon, Cellulose: a random walk along its historical path, Cellulose 1 (1994) 1–25.
[24] M.C. Hwang, K.M. Chen, Removal of color from effluents using polyamide-epichlorohydrin-cellulose polymer II: use in acid dye removal, J. Appl. Polym. Sci. 49 (1993) 975–989.
[25] A. Hashem, R.M. EI-Shishtawy, Preparation and characterization of cationized cellulose for the removal of anionic dyes, Adsorpt. Sci. Technol. 19 (2001) 197–210.
[26] X. Guo, Y. Du, F. Chen, H.S. Park, Y. Xie, Mechanism of removal of arsenic by bead cellulose loaded with iron oxyhydroxide (β-FeOOH): EXAFS study, J. Colloid Interface Sci. 314 (2007) 427–433.
[27] E. Mištová, H. Parschová, Z. Matějka, Selective sorption of metal oxoanions from dilute solution by bead cellulose sorbent, Sep. Sci. Technol. 42 (2007) 1231–1243.
[28] J. Cai, L. Zhang, Unique gelation behavior of cellulose in NaOH/urea aqueous solution, Biomacromalecules 7 (2006) 183–189.
[29] J. Cai, L. Zhang, J. Zhou, H. Qi, H. Chen, T. Kondo, X. Chen, B. Chu, Multifilament fibers based on dissolution of cellulose in NaOH/urea aqueous solution: structure and properties, Adv. Mater. 19 (2007) 821–825.
[30] S. Liu, L. Zhang, J. Zhou, J. Xiang, J. Sun, J. Guan, Fiberlike Fe_2O_3 macroporous nanomaterials fabricated by calcinating regenerate cellulose composite film, Chem. Mater. 20 (2008) 3623–3628.
[31] X. Luo, L. Zhang, S. Liu, J. Zhou, In situ synthesis of Fe_3O_4/cellulose microspheres with magnetic-induced protein delivery, J. Mater. Chem. 19 (2009) 3538–3545.
[32] R. Massart, Preparation of aqueous magnetic liquids in alkaline and acidic media, IEEE Trans. Magn. 17 (1981) 1247–1248.
[33] Y. Wu, Y. Xiao, Y. Zhou, Micromixing in the submerged circulative impinging stream reactor, Chin. J. Chem. Eng. 4 (2003) 420–425.
[34] H. Brauer, Development and performance of stagnation jet mixer, Ger. Chem. Eng. 4 (1981) 144–154.
[35] Y. Wu, Impinging Streams Fundamentals, Properties and Application, Elsevier, Amsterdam, 2006.
[36] R. Chi, Z. Xu, Y. Wu, C. Wang, Optimal conditions for preparing ultra-fine CeO_2 powders in a submerged circulative impinging stream reactor, J. Rare Earth 25 (2007) 422–427.
[37] G. Fundueanu, C. Nastruzzi, A. Carpov, J. Desbrieres, M. Rinaudo, Hysico-chemical characterization of Ca-alginate microparticles produced with different methods, Biomaterials 20 (1999) 1427–1435.

[38] A. Blandino, M. Macias, D. Cantero, Formation of calcium alginate gel capsules: influence of sodium alginate and CaCl$_2$ concentration on gelation kinetics, J. Biosci. Bioeng. 88 (1999) 686–689.

[39] H. Pilgrimm. Superparamagnetic particles, process for their manufacture and usage, US Patent 5,928,958 (July 27, 1999).

[40] D.K. Rassis, I.S. Saguy, A. Nussinovitch, Collapse, shrinkage and structural changes in dried alginate gels containing fillers, Food Hydrocolloids 16 (2002) 139–151.

[41] J. Bird, N. Brough, S. Dixon, N. Batchelor, Understanding adsorption phenomena: investigation of the dye–cellulose interaction, J. Phys. Chem. B 110 (2006) 19557–19561.

[42] J.H.P. Watson, B.A. Cressey, A.P. Roberts, D.C. Ellwood, J.M. Charnock, A.K. Soper, Structural and magnetic studies on heavy-metal-adsorbing iron sulphide nanoparticles produced by sulphate-reducing bacteria, J. Magn. Magn. Mater. 214 (2000) 13–30.

[43] Y.S. Ho, G. McKay, Sorption of dyes and copper ions onto biosorbents, Process. Biochem. 38 (2003) 1047–1061.

[44] G. Bayramoglu, A. Denizli, S. Bektas, M.Y. Arica, Entrapment of Lentinus sajor-caju into Ca-alginate gel beads for removal of Cd(II) ions from aqueous solution: preparation and biosorption kinetics analysis, Microchem. J. 72 (2002) 63–67.

[45] R.E. Treybal, Mass-Transfer Operations, third ed., McGraw-Hill international, Singapore, 1981.